Hepatic Cdkal1 deletion enhances cholesterol efflux capacity with regulation of HDL metabolism

Dan Bi An

The Graduate School Yonsei University

The Graduate Program of Biomedical Engineering

Hepatic Cdkal1 deletion enhances cholesterol efflux capacity with regulation of HDL metabolism

Supervised by Professor Sang-Hak Lee

The Doctoral Dissertation submitted to
the Department of Graduate Program
in Biomedical Engineering,
the Graduate School of Yonsei University
in partial fulfillment of the requirements
for the degree of Doctor of Biomedical Engineering

Dan Bi An

December 2022

This certifies that the doctoral dissertation of

Dan Bi An is approved.

Thesis Supervisor: Sang Hak Lee

Thesis Committee Member #1: Jae Woo Song

Thesis Committee Member #2: Jung Sun Kim

Thesis Committee Member #3: Chan Joo Lee

Thesis Committee Member #4: Yong Ho Lee

The Graduate School

Yonsei University

December 2022

ACKNOWLEDGEMENTS

박사과정을 무사히 마칠 수 있기까지 많은 분들의 도움이 있었습니다. 이 글을 통해 그분들에게 감사의 인사를 전해 드리고자 합니다.

먼저 박사과정 동안 연구에 매진할 수 있도록 아낌없는 격려와 지도를 해주신 이상학학교수님께 진심으로 깊은 감사를 드립니다. 바쁘신 중에도 논문의 심사와 진심 어린 조언을 해주신 송재우교수님, 김중선교수님, 이찬주교수님, 이용호교수님께도 깊은 감사의 마음을 전합니다. 교수님들의 가르침을 바탕으로 올바른 연구자가 될 수 있도록 노력하겠습니다.

또한 부족한 저에게 많은 것을 가르쳐 주시고 따뜻한 배려와 조언을 해주신 안수진교수님, 연구 데이터 통계분석에 힘써주신 박정미선생님과 강유라선생님, 실험실에 처음 들어왔을 때부터 함께 연구하고 한결같이 저를 챙겨줬던 재호, 유리, 하린이, 승민이, 현지에게도 고마움을 전합니다. 그리고 같은 실험실에서 응원해주시고 챙겨주신 채민경선생님과 최진옥선생님께도 감사의 인사를 전합니다.

사회에서 만나 항상 저에게 많은 힘이 되고 응원해 주었던 현주언니와 같은 학위과정에서 언제나 내 편이 되어준 수연언니에게 고마움을 전합니다.

마지막으로 저를 항상 믿고 배려해주시고 늦은 학교생활을 뒷바라지 해주신 부모님과 보슬이에게 진심으로 감사드립니다.

안단비 올림

TABLE OF CONTENTS

ABSTRACT ····· 1

I. INTRODUCTION ····· 3

II. MATERIALS AND METHODS

2.1. Animals and cells····· 7

2.2. Biochemical analyses ····· 9

2.3. Cholesterol efflux assay (CEC)····· 10

2.4. Enzyme activity assays ····· 12

2.5. Western blotting ····· 13

2.6. Atherosclerotic plaque assessment ····· 14

2.7. RNA sequencing and analysis of differentially expressed genes ··· 15

2.8. Statistical Analysis····· 16

III. RESULTS

3.1. Generation of liver-specific *Cdkal1* KO mice and *Apoe/Cdkal1* KO mice ····· 17

3.2. Metabolic parameters of *Cdkal1* KO mice ····· 22

3.3. Effect of *Cdkal1* deletion on CEC and atherosclerosis ····· 24

3.4. Effect of *Cdkal1* deletion on regulation of HDL metabolism ····· 30

3.5. Differentially expressed genes and related pathways ····· 36

IV. DISCUSSION ····· 39

V. REFERENCES ····· 43

ABSTRACT (IN KOREAN) ····· 53

LIST OF FIGURES

Figure 1. Schematic diagram showing the procedure of the cholesterol efflux experiment ····· 11

Figure 2. Generation of liver-specific *Cdkal1* KO mice ····· 20

Figure 3. Generation of *Apoe/Cdkal1* KO mice for atherosclerosis model ····· 22

Figure 4. Circulating glucose and lipid profile ····· 24

Figure 5. Increased CEC in *Cdkal1* KO mice ····· 27

Figure 6. Increased CEC in *Apoe/Cdkal1* KO mice ····· 28

Figure 7. Atherosclerotic plaque assessment ····· 29

Figure 8. Enzyme activity in *Cdkal1* ····· 33

Figure 9. Hepatic *Cdkal1* deletion regulates SR-B1, EL, and HL protein expression ····· 34

Figure 10. Correlation between CEC and proteins involved in HDL metabolism····· 36

Figure 11. Analysis of RNA sequencing of liver-specific *Cdkal1* mice ····· 38

ABSTRACT

Hepatic Cdkal1 deletion enhances cholesterol efflux capacity with regulation of HDL metabolism

Dan Bi An

Graduate Program in Biomedical Engineering

The Graduate School, Yonsei University

(Directed by Professor Sang-Hak Lee)

Previous studies have reported that individuals with *CDKAL1* variants were associated with promoted cholesterol efflux capacity (CEC) by genome-wide association studies (GWAS). In this study, we investigated the effect of liver-specific deletion of *Cdkal1* on mouse CEC and atherosclerosis.

In this study, liver-specific *Cdkal1* gene-deleted mouse was prepared and blood, CEC,

high density lipoprotein (HDL) metabolism-related protein, and RNA-seq were identified. To confirm the direct effect on atherosclerosis, double knockout (KO) mice were produced by crossing *Apoe* KO and liver-specific *Cdkal1* KO mice.

CEC was higher in *Cdkal1* KO mice than in wild-type (WT) mice ($p = 0.007$) and higher in *Apoe*/*Cdkal1* KO mice than in *Apoe* KO mice ($p = 0.034$). Serum enzyme activities of LCAT, PLTP, and LPL were similar between WT and *Cdkal1* KO mice. Liver tissue western blotting revealed reduced EL ($p = 0.002$), HL ($p < 0.001$) and elevated SR-B1 ($p = 0.007$) in *Cdkal1* KO mice. In the high cholesterol diet-induced atherosclerosis model, atherosclerotic plaques tended to decrease in the *Cdkal1* KO group, but there was no significant difference ($p = 0.067$). As a result of comparative analysis of hepatocytes from *Cdkal1* KO mice and those from WT mice by RNA sequencing, it was confirmed that the bile secretion pathway was upregulated.

The current study demonstrated that CEC is promoted in mice with liver-specific deletion of *Cdkal1* with regulation of proteins for HDL metabolism. This study suggests *CDKAL1* could be a target of intervention to improve HDL function and vascular pathology.

Key words: atherosclerosis, macrophage, liver, plaque

Hepatic Cdkal1 deletion enhances cholesterol efflux capacity with regulation of HDL metabolism

Dan Bi An

Graduate Program in Biomedical Engineering

The Graduate School, Yonsei University

(Directed by Professor Sang-Hak Lee)

I. INTRODUCTION

In previous research, the relationship between low high-density lipoprotein-cholesterol

(HDL-C) levels and coronary heart disease risk has been well reported [1,2]. However, the uncertain effects of HDL-C in some genetic studies [3] and failure of HDL-C-raising drugs to protect against coronary heart disease [4] have triggered debate on the beneficial effects of HDL and HDL-C levels. Conversely, very recent genetic studies analyzing characteristics of HDL particles revealed a protective effect against coronary artery disease [5]. The HDL particle size can be divided into large (9.4–14.0 nm), medium (8.3–9.3 nm) and small (7.3–8.2 nm) [6]. Of these HDL subpopulations, large size HDL levels show an inversely proportional relationship with cardiovascular risk in univariate analysis, while concentrations of small HDL particles generally show a positive correlation with risk [7–9].

Furthermore, many researchers and physicians are still interested in the influence of therapeutics based on HDL and reverse cholesterol transport (RCT) on vascular disease [10,11]. RCT, an important part of cholesterol metabolism in the body, is a process that absorbs cholesterol from peripheral organs, exchanges cholesterol for triglycerides in the blood, and finally delivers cholesterol to the liver, where it is disassembled and excreted [12]. The efflux of unesterified cholesterol is the first and rate-limiting step of RCT.

A previous study reported an association between *CDKAL1* variants and cholesterol efflux capacity (CEC) using a human genome-wide association and replication study. In that study, 631 variants were associated in the discovery set, whereas five of which, including four near *CDKAL1*, were associated with CEC in the replication set [13]. Based on these results, we aimed to investigate the pathways by which *Cdkal1* affects CEC, and whether this gene

influences atherosclerosis.

In prior studies, genetic variants of *Cdkal1* (Cdk5 regulatory subunit associated protein 1-like 1) were linked to impaired insulin response and the risk of type 2 diabetes mellitus in diverse ethnicities [14]. As a mammalian methylthiotransferase, *Cdkal1* has been reported to catalyze modification of tRNA needed in protein translation [10]. However, no study to date has reported its effects on HDL metabolism or related parameters.

HDL metabolism includes the interaction of factors controlling synthesis, lipase-induced vascular remodeling, and catabolism. The interaction of HDL with cellular receptors and plasma proteins, including endothelial lipase (EL), hepatic lipase (HL), scavenger receptor class B type I (SR-BI), lipoprotein lipase (LPL), lecithin–cholesterol acyltransferase (LCAT), phospholipid transfer protein (PLTP), and ATP binding cassette transporter 1 (ABCA1), results in HDL remodeling and catabolism [15]. Even though inhibition of EL function increased plasma HDL levels [16,17], and scavenger receptor, class B type 1 (SR-B1) mediates the efflux of excess cholesterol in other cells [18], still the association of these proteins with *CDKAL1* has not been reported.

Therefore, the aim of this study was to investigate the effect of *Cdkal1* deficiency associated with CEC on HDL metabolism, as well as atherosclerosis and its underlying mechanisms. Liver-specific *Cdkal1* knockout (KO) mice were generated, and lipid profiles, CEC were compared in *Cdkal1* KO and wild-type (WT) mice. In addition, aortic atherosclerosis was compared in *Apoe/Cdkal1* double KO and *Apoe* KO mice fed high-fat diets. To elucidate associated biological pathways, regulatory effects on target molecules

involved in HDL metabolism were assessed.

II. MATERIALS AND METHODS

2.1. Animals and cells

Cdkal1 KO mice were generated by crossing *Cdkal1* flox/flox mice (From Prof. Tomizawa in Kumamoto University) with *Albumin-Cre* recombinase transgenic mice (The Jackson Laboratory; Stock No. 003574). *Apoe*/*Cdkal1* KO mice were generated by crossing *Cdkal1* KO mice with *Apoe* mice (The Jackson Laboratory, Stock No. 002052). All mice were maintained in a controlled environment with 12 h cycle light/dark (dark cycle, 6 PM to 6 AM), and the temperature was kept at 22 °C in individually ventilated cages (Animal Care Systems) and received free access to a standard chow diet (Harlan Teklad;2918) and water.

For atherosclerosis studies, 5week old *Apoe*/*Cdkal1* KO mice were fed atherogenic high-cholesterol diet (HCD) (Purified diet matched to Paigen's atherogenic rodent diet; D12336 from Research diets) for 16weeks. Body weight and food intake were weekly assessed during the duration of the study and no important adverse events were observed. All experiments were performed according to protocols approved by the Institutional Animal Care and Use Committee, Yonsei University College of Medicine, Seoul, Korea (YUHS-IACUC: Yonsei University Health System Institutional Animal Care and Use Committee).

Blood was obtained from each animal at the time of death for analysis of circulating lipid profile and in vitro cholesterol efflux test. After an overnight fast, blood samples were

collected from the abdominal vena cava and serum samples were allowed to clot for 30 min at room temperature before serum and plasma separation by centrifugation (3000 rpm for 30 min at 4 °C). Serum samples were used for chemical assays within 3 days, and aliquots were stored at − 80 °C for determination of the cellular cholesterol efflux.

Macrophage cell lines J774 cells were provided by Professor Yury Miller of the university of California Diego, CA, USA. J774 mice macrophages were cultured in DMEM medium supplemented with 10% FBS (Fetal Bovine Serum) and 1% antibiotic-antimycotic. The cells were incubated at 37 °C in 5% CO^2 environment. [^{3}H] cholesterol treatment and culture of [^{3}H] cholesterol labeled cells was performed in the radioisotope management area.

2.2. Biochemical analyses

Serum total cholesterol, HDL cholesterol, LDL cholesterol, triglyceride and glucose levels were requested for analysis by KBIO Health, Cheong-ju, Korea.

Before starting the test, quality control was completed with standard materials suitable for each reagent. The sample was delivered and quickly vortex mixed to prevent the formation of a concentration gradient, and the following items were measured with an automatic biochemical analyzer (Konelab PRIME 60i, Thermo scientific, FIN).

2.3. Cholesterol efflux assay

Cellular cholesterol efflux was determined by using the J774 cells according to a previously described procedure [19, 22]. Briefly, J774 cells were plated on 24-well plates at $4x10^4$ cells/well and cholesterol labeled by incubation for 24 h in serum free DMEM with containing 1 μCi of [^{3}H] cholesterol. The cells were then maintained for 2h in DMEM supplemented with 0.2% BSA in the presence of 0.3mM of cAMP (Santa Cruz Biothechnology, sc-201569A) and 2μg/ml of ACAT inhibitor (ChemCruz, sc-215839). Then, after removing the existing media, ACAT and 20μl/ml serum were treated and incubated for 4 hours. After incubation, supernatant was collected, washed with PBS and then the cells were harvested. Radioactivity in both media and cells was determined by liquid scintillation counting using a beta counter. Total cellular [^{3}H] cholesterol was calculated as the sum of the radioactivity of the cells, and this was used to calculate the [^{3}H] cholesterol efflux.

Cholesterol efflux was calculated as:

([^{3}H] cholesterol in medium/([^{3}H] cholesterol in medium+[^{3}H] cholesterol in cells)×100) [22].

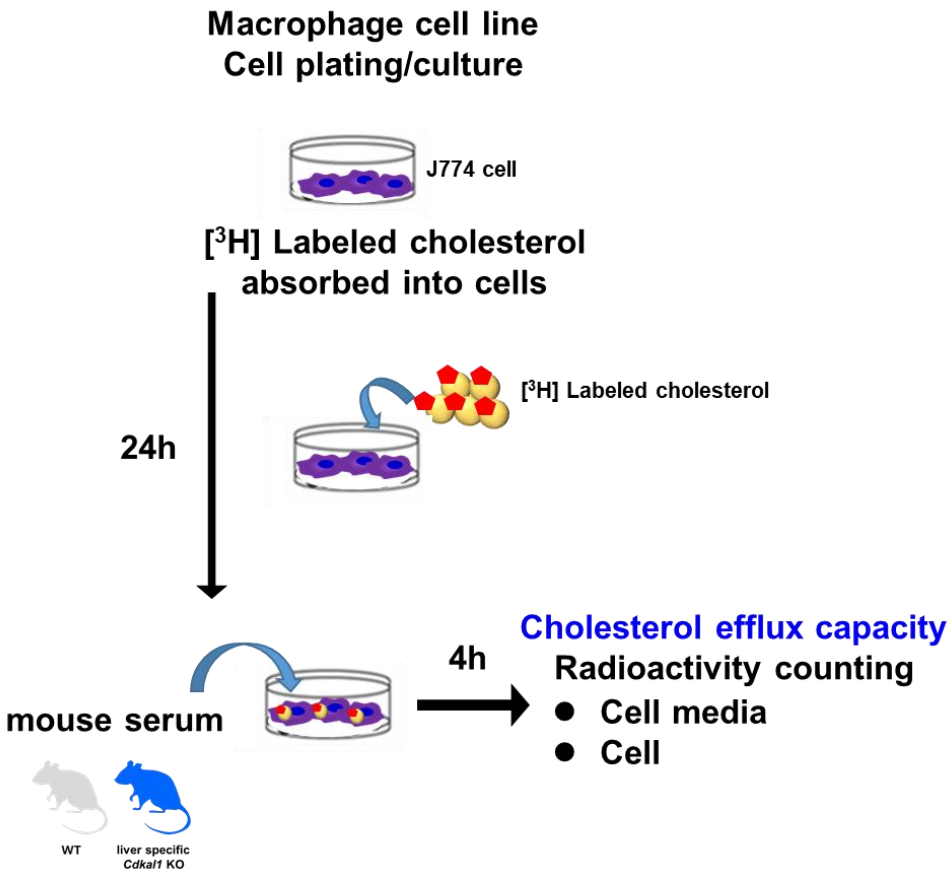

Figure 1. Schematic diagram showing the procedure of the cholesterol efflux experiment. Incubate macrophages with radiolabeled cholesterol for 24 hours. Serum free of apolipoprotein-B (ApoB) particles using precipitation is applied to the cells. After 4 hours, the cells and media are harvested separately and then the cholesterol efflux capacity is expressed as a percentage using a formula.

2.4. Enzyme activity assays

LPL, PLTP, LCAT activity assay was determined by an activity assay kit (Fluorometric) (LPL (Abcam, ab204721), PLTP (Abcam, ab196998), LCAT (EMD, Cat.428900)) in plasma of the mice following the manufacturer's instructions.

2.5. Western blotting

Liver tissues were washed in cold PBS, and homogenized in PBS containing the protease inhibitor cocktail (Fermentas) and phosphatase inhibitor cocktail (Roche). The lysates were spun down at 4°C (14,000rpm) for 15 minutes, and the supernatant was collected. Protein quantification was done by BCA assay (Pierce™ BCA Protein Assay Kit, Thermo Scientific™, #23227). Equal amount of total protein was subjected to electrophoresis on 10% SDS-PAGE (Sodium dodecyl sulfate polyacrylamide) gel and transferred to Polyvinylidene fluoride (PVDF) membranes by using a Bio-Rad Western blotting system (Mini-Protean® Tetra Cell Mini Trans-Blot module; Bio-Rad Laboratories, Hercules, CA, USA). Membranes were blocked with 5% fat-free milk containing 0.1% Tween 20 for 1hour at room temperature and incubated with primary antibody (CDKAL1 (Abcam, Ab169531), EL (Boster, A01020), HL (Abcam, Ab175105), SR-B1(Abcam, Ab217318), ABCA1 (Abcam, Ab18180)) overnight at 4°C. Membranes were then incubated with HRP-conjugated secondary antibodies (Santa Cruz Biothechnology, sc-2357, sc-516102). Following washing in tris-buffered saline containing 0.1% Tween-20 (TBST) for 10 min thrice, the blots were visualized and imaged using ECL Plus Kit (Millipore Corporation, Billerica, MA) and Image Quant™ LAS 4000 (GE Healthcare). The proteins were normalized with β-actin (Santa Cruz Biothechnology, sc-47778) and respective total protein content. Densitometry quantification of protein expression was performed using Image J.

2.6. Atherosclerotic plaque assessment

Before sacrificing, mice were anesthetized Zoletil mix with Rompun (4:1). The concentration is 20 mg/kg. Post perfusion, the aorta was segmented and following careful removal of surrounding extraneous fat and connective tissue, it was dissected longitudinally and fixed in 4% (w/v) paraformaldehyde for en face lesion analysis. To measure the percent of atherosclerosis, dissected aorta were pinned resin and stained with Oil Red O (60% (v/v) in isopropanol). En face lesion area was measured by Images were taken with a stereo microscope digital camera (Leica, m205) and analyzed by computer-assisted image analysis (image J).

2.7. RNA sequencing and analysis of differentially expressed genes

Livers were harvested from WT and *Cdkal1* KO mice (5-week-old, n=3 for each group) and rinsed in Hanks' Balanced Salt Solution (Millipore Sigma, Burlington, MA, USA). After collagenase treatment, the supernatant was carefully decanted, and hepatocyte growth medium (PromoCell, Heidelberg, Germany) supplemented with 10% foetal bovine serum was added. These were filtered through a 70-μm pore nylon cell strainer and centrifuged for hepatocyte isolation.

100 ng RNA was used for cDNA synthesis using an iScript cDNA synthesis kit (Bio-Rad Laboratories, Hercules, CA, USA). RNA purity was determined by assaying on a Nano Drop 8000 spectrophotometer (Thermo Fisher Scientific, Waltham, MA, USA). Total RNA integrity was checked using an Agilent Technologies 2100 Bioanalyzer (Agilent Technologies, Inc., Santa Clara, CA, USA). Total RNA sequencing libraries were prepared according to the manufacturer's instructions (Illumina Standard Total RNA Sample prep kit with Ribo-zero Human/mouse/rat reagent; Illumina, Inc., San Diego, CA, USA). A total of 400 ng RNA was subjected to ribosomal RNA depletion with Ribo-zero reagent using biotinylated probes that selectively bind rRNA. Following purification, rRNA-depleted RNA was fragmented using divalent cations under elevated temperature. The cleaved RNA fragments were copied into first-strand cDNA using reverse transcriptase and random primers. This was followed by second-strand cDNA synthesis using DNA polymerase I and RNase H. Single 'A' bases were added, and adapters were ligated. The products were

purified and enriched using PCR to create a final cDNA library. After qPCR, index-tagged cDNA libraries were combined in equimolar amounts. RNA sequencing was performed using an Illumina NovaSeq 6000 system according to the provided protocol for 2×100 sequencing (Illumina).

After successful test to calculate gene expression level, two-fold change was calculated, and genes belonging to the range (|log2 FC| ≥1) were selected. DEGs were analysed using the DAVID software (https://david.ncifcrf.gov/). KEGG pathway statistics were used to identify pathways for analysis.

2.8. Statistical analysis

All graphs were plotted with GraphPad Prism 5 (GraphPad Software Ltd, La Jolla, CA, USA) and values are shown as the mean ± standard deviation. In the figure, the results are expressed as mean±SEM. The differences among the groups of subjects were evaluated by Permutation test. Significance was accepted at $p<0.05$ and $p<0.01$. Statistical analyses were performed with PASW Statistics version 18.

III. RESULTS

3.1. Generation of liver-specific *Cdkal1* KO mice and *Apoe/Cdkal1* KO mice

For experiments to determine how deficiency of the *Cdkal1* gene affects cholesterol metabolism, we generated a mouse model in which the *Cdkal1* gene was specifically deleted from the liver (hereafter referred to as *Cdkal1* KO), the central organ of cholesterol metabolism. *Cdkal1* KO mice were generated by crossing *Cdkal1*$^{fl/fl}$ mice with *Albumin-Cre* mice. These mice induced ablation of the *Cdkal1* region by *Albumin-Cre* recombinase activity at the *floxP* site of *Cdkal1*$^{fl/fl}$ mice, resulting in liver-specific *Cdkal1* knockout mice (Fig. 2A). DNA was extracted from the toe tissue of 2-week-old mice and the genotype was confirmed by PCR amplification. *Cdkal1* gene was identified at 350 bp in 6% agarose gels and *Albumin-Cr*e gene at 100 bp in 9% agarose gels. The absence of *Cdkal1* gene expression and the presence of *Alb-Cre* gene in the *Cdkal*1 KO group confirmed that the *Cdkal1* gene was removed from the liver (Fig. 2B). Mice were weighed weekly from 5 weeks to 16 weeks of age. As a result, it was confirmed that there was no significant difference in body weight of the *Cdkal1* KO group compared with that of the WT (Fig. 2C). There was no change in survival between the *Cdkal1* KO and the WT groups from 5 weeks of age until sacrifice after the end of the experiment, and there was no difference in food and water intake during the experimental period. Therefore, it was confirmed that the

deletion of the *Cdkal1* gene in liver tissue did not cause severe sequelae.

Next, we generated *Apoe/Cdkal1* KO mice to determine how inhibition of *Cdkal1* in the liver affects atherosclerosis. *Cdkal1* KO mice were generated in the same manner as shown in Figure 2A, and then crossed with *Apoe* KO mice to produce whole-body *Apoe* KO liver-specific *Cdkal1* KO mice. DNA was extracted from the toe tissues of 2-week-old mice, and the genotype was confirmed by PCR amplification. As expected, it was confirmed that *Apoe/Cdkal1* KO mice were generated (Fig. 3A). As a control group, *Apoe* KO/*Cdkal1*$^{fl/fl}$ (*Apoe* KO) mice were generated and used in the experiment (Fig. 3A). For the atherosclerosis model, 5-week-old *Apoe/Cdkal1* KO and *Apoe* KO mice were fed high cholesterol diet (HCD) (D12336 from Research diets) for 16 weeks, and body weights were measured weekly until the end of the experiment. There was no difference in body weight between the *Apoe/Cdkal1* KO and *Apoe* KO groups (Fig. 3B). HCD was replaced with a new one every 2 days, and there was no difference between groups in diet, water intake, and survival.

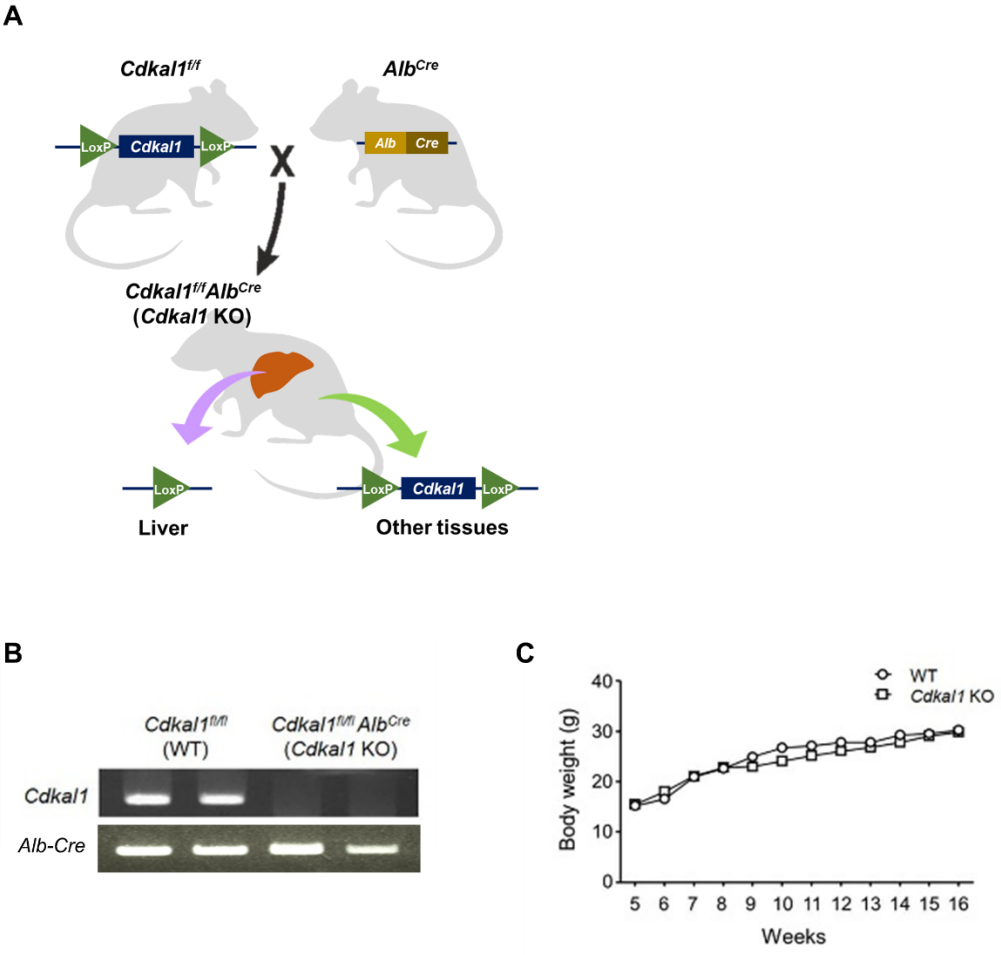

Figure 2 legend (the following page)

Figure 2. Generation of liver-specific *Cdkal1* KO mice. (A) Schematic showing the generation of liver-specific *Cdkal1* knockout mice. Liver-specific *Cdkal1* KO mouse was generated by crossing a *Cdkal1*$^{fl/fl}$ mice having a *floxP* site in the *Cdkal1* gene with an *Alb-Cre* mouse having an *Albumin-Cre* site. (B) *Cdkal1* KO mice genotyping was performed by PCR. Mice tail DNA was amplified with primers for *Cdkal1*. PCR products were separated on 6% agarose gels (350 bp), with primers for the *Alb-Cre* PCR product isolated on a 9% agarose gel (100 bp). (C) Body weight graph measured weekly from 5 to 16 weeks of age in *Cdkal1* KO and WT groups (n = 12 each). Results were presented with mean ± SEM. Statistical analysis by permutation test.

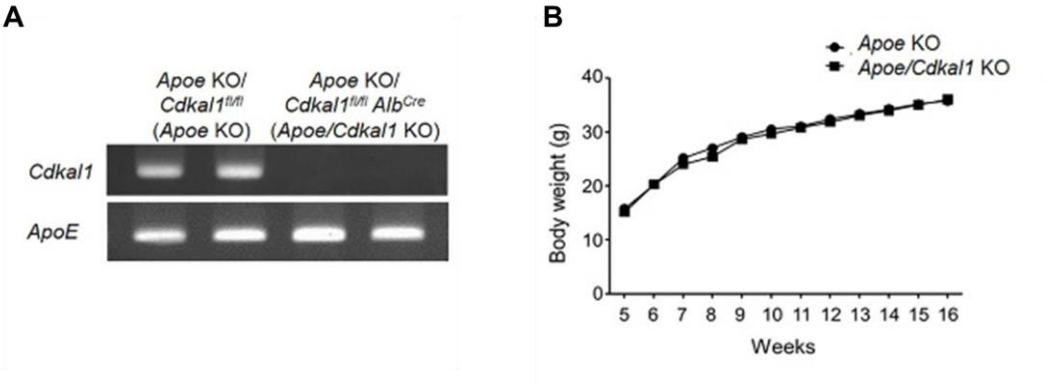

Figure 3. Generation of *Apoe/Cdkal1* KO mice for atherosclerosis model.

(A) *Apoe/Cdkal1* KO mice genotyping was performed by PCR. Mice tail DNA was amplified with primers for *Cdkal1*. PCR products were separated on 6% agarose gels (350bp) with primers for the *Apoe* PCR product separated on a 9% agarose gel (200 bp). (B) Weekly weight graphs from 5 to 16 weeks in the *Apoe/Cdkal1* KO and the *Apoe* KO groups fed the HCD diet (n = 12 each). Results were presented with mean ± SEM. Statistical analysis by permutation test.

3.2. Metabolic parameters of *Cdkal1* KO mice

Next, we investigated whether *Cdkal1* deficiency affects key plasma parameters of metabolic dysfunction. Before the experiment, the mice were fasted overnight. Blood were sampled from the veins of 8-week-old WT and *Cdkal1* mice and stored at room temperature for 30 min. Then, the serum sample was obtained by centrifugation at 3000 rpm for 30 min at 4 °C, and analysis was requested from KBIO Health. As a result, serum total cholesterol, HDL cholesterol, LDL cholesterol, triglyceride, and glucose levels in *Cdkal1* mice were similar ($p > 0.05$) to those in WT mice (Figure 4). These findings confirmed that liver *Cdkal1* deficiency did not affect the circulating lipid profile of mice.

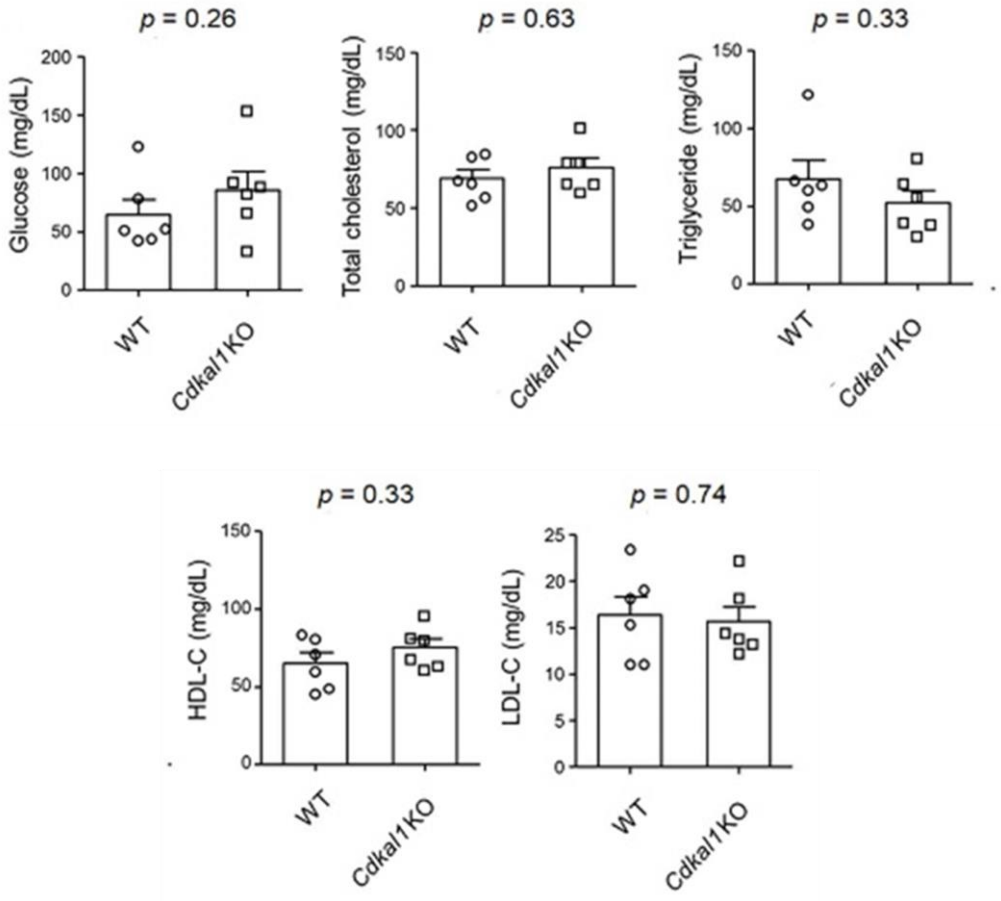

Figure 4 legend (the following page)

Figure 4. Circulating glucose and lipid profile. Plasma lipid and glucose measurements. Fasting plasma total cholesterol, HDL cholesterol, LDL cholesterol, triglyceride and glucose levels in 8-week-old *Cdkal1* KO mice (compared with WT, n = 6 in each group). Results were presented with mean ± SEM. Statistical analysis by permutation test.

3.3. Effect of *Cdkal1* deletion on CEC and atherosclerosis

We obtained serum from 8-week-old *Cdkal1* KO mice and tested for cholesterol efflux with J774 macrophages labeled with [^{3}H] cholesterol. J774 cells were seeded one day before and maintained in serum free Dulbecco's modified Eagle medium containing 1 μCi/mL of [^{3}H] cholesterol for 24 h. Then, after treatment with serum, cells and supernatants were collected and measured with a beta counter after 4 h. As expected by the deficiency of *Cdkal1*, we observed an increase in cholesterol efflux in *Cdkal1* KO serum (p = 0.007 versus WT mice; Fig. 5). These findings confirmed that hepatic *Cdkal1* deficiency induces improved cholesterol efflux.

To confirm that the effect of promoting cholesterol efflux in *Cdkal1* KO mice was repeated in *Apoe/Cdkal1* KO mice, an *in vitro* cholesterol efflux experiment was performed with serum from 8-week-old *Apoe/Cdkal1* KO and *Apoe* KO mice. After the J774 cells were labeled with [^{3}H] cholesterol for one day, the serum was treated, and the cells and supernatant were obtained after 4 h. Then, the sample mixed with the cocktail buffer was measured with a beta counter. As expected, within the *Apoe/Cdkal1* KO group, cholesterol efflux was promoted compared to *Apoe* KO group. (p = 0.034; Fig. 6). These results suggest that deletion of *Cdkal1* has a positive effect on cholesterol efflux even in mice with reduced *Apoe* gene, which is known to induce atherosclerosis by metabolic dysfunction.

The aorta tissues obtained from KO mice and those fed an HCD for 16 weeks were stained with Oil Red O. It was confirmed that the HCD-induced atherosclerosis model was

completed with the aorta Oil Red O-stained image of *Apoe* KO mice (Fig. 7A). We found that the mean lesion area of the aorta tended to be in *Apoe/Cdkal1* KO mice ($p = 0.067$) than in *Apoe* KO mice, but no significant difference could be identified (Fig. 7B).

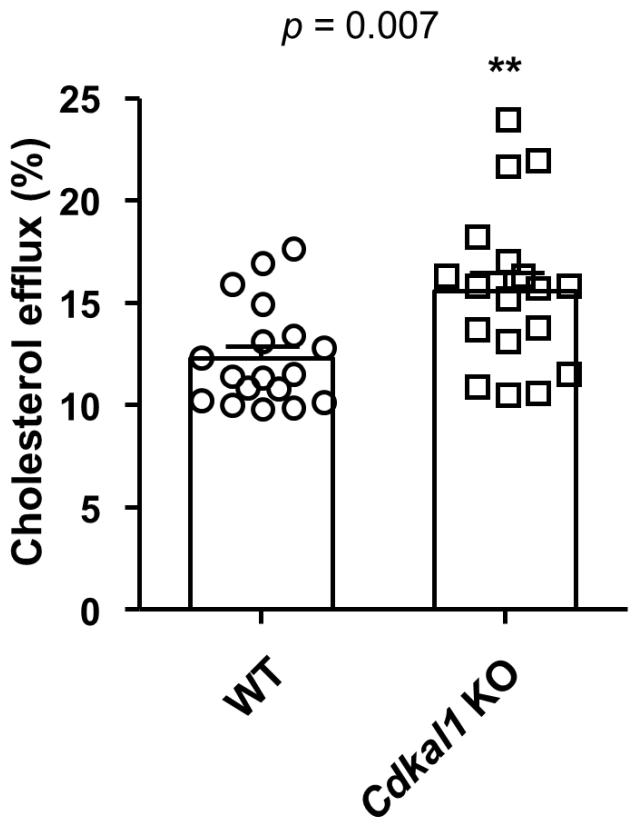

Figure 5. Increased cholesterol efflux in serum *Cdkal1* KO mice. [^{3}H] cholesterol efflux capacity in comparison with *Cdkal1* KO and WT mice (n = 18 in each group). [^{3}H] cholesterol labeled cells were incubated with 20 μL/mL serum for 4 h. Cholesterol efflux was expressed as radioactivity in the supernatant relative to total radioactivity (in supernatant and cells). Values shown represent means of two individual experiments performed in duplicate. Results were presented with mean ± SEM. $^{**}p < 0.01$ compared with WT (permutation test).

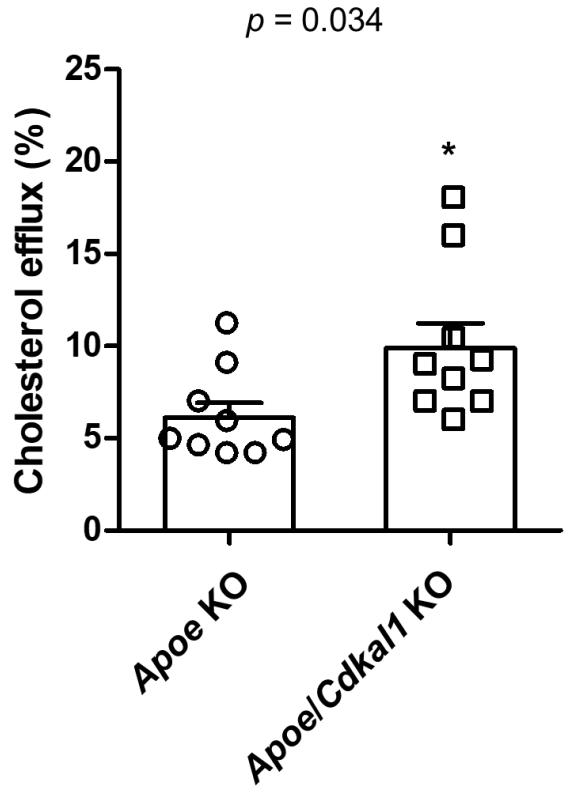

Figure 6. Increased cholesterol efflux in serum *Apoe/Cdkal1* KO mice. [^{3}H] cholesterol efflux capacity in comparison with *Apoe/Cdkal1* KO and *Apoe* KO mice (n = 9 in each group). [^{3}H] cholesterol labeled cells were incubated with 20 μL/mL serum for 4 h. Cholesterol efflux was expressed as radioactivity in the supernatant relative to total radioactivity (in supernatant and cells). Values shown represent means of two individual experiments performed in duplicate. Results were presented with mean ± SEM. *$p < 0.05$ compared with *Apoe* KO mice (permutation test).

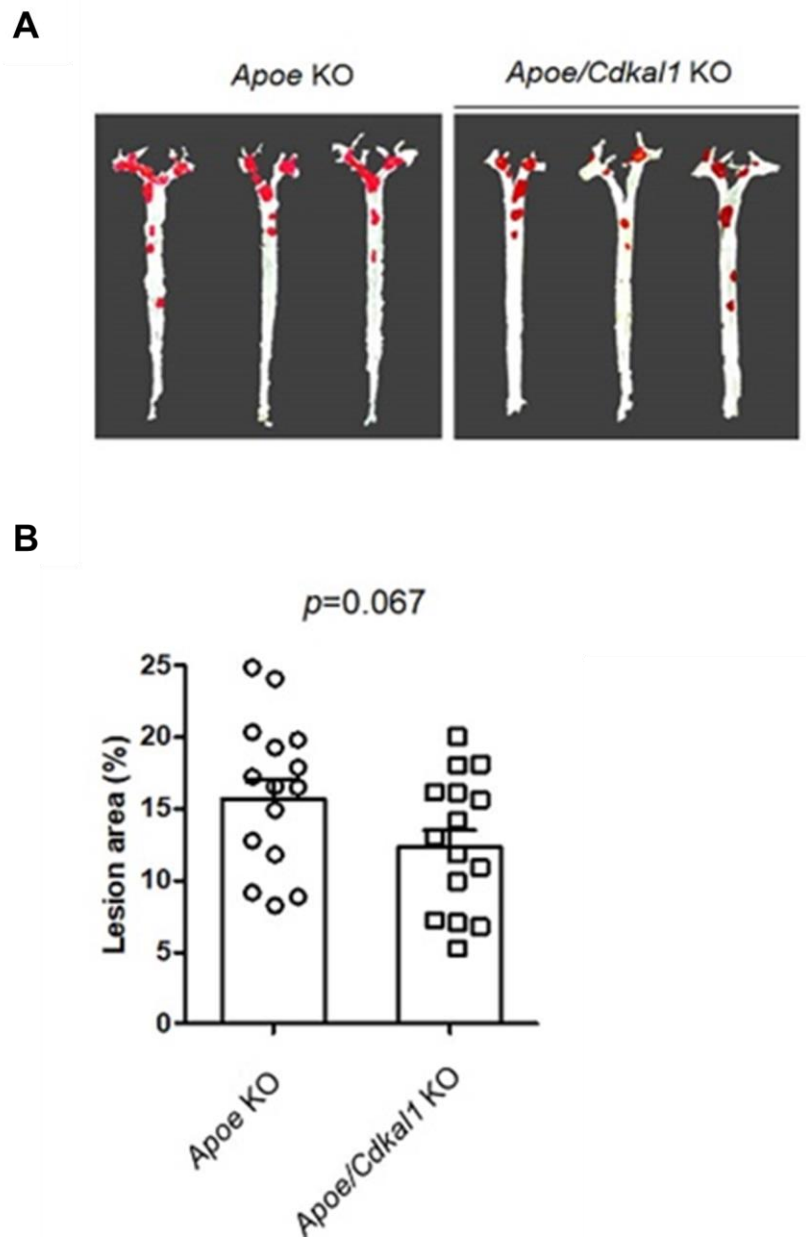

Figure 7 legend (the following page)

Figure 7. Atherosclerotic plaque assessment.

Cdkal1 deficiency in *Apoe* KO mouse livers attenuated atherosclerotic plaque formation. Male *Apoe/Cdkal1* KO mice and *Apoe* mice were fed HCD for 16 weeks. (A) typical micrograph of Oil Red O staining of en face aorta, and (B) data obtained by quantifying the lesion size using Image J (n=15 in each group). Results were presented with mean ± SEM. (permutation test).

3.4. Effect of *Cdkal1* deletion on regulation of HDL metabolism

To determine whether these results are the effect of HDL catabolism, which plays an important role in cholesterol efflux, we investigated whether the reduction of *Cdkal1* deletion in the liver affects the enzymatic activity. LCAT and PLTP, which are enzymes that enhance the cholesterol-removing ability of HDL, convert HDL into a mature form and help move phospholipids to the surface membrane, respectively. As a result of confirming the activity of LCAT and PLTP with plasma from *Cdkal1* KO and WT mice, it was confirmed that there was no difference between the two groups ($p > 0.05$; Fig. 8). LPL activity, which is known to help hydrolyze triglycerides of apolipoprotein B (ApoB)-containing lipoproteins to be absorbed into muscle or adipose tissues, also showed no significant change between *Cdkal1* KO and WT mice ($p > 0.05$; Fig. 8). These results suggest that deletion of the *Cdkal1* gene in the liver does not promote CEC through the enzyme.

Next, to investigate how CEC alterations in mice with liver-specific *Cdkal1* deletion were mediated, we checked expression of HDL catabolism-related proteins in *Cdkal1* KO mice [21]. After protein extraction from liver tissues of 8-week-old *Cdkal1* KO and WT mice, the protein level was confirmed by western blot analysis. First, we checked the CDKAL1 protein level to check that the liver-specific *Cdkal1* deleted mice. As a result, it was confirmed that CDKAL1 protein was not expressed in the liver of *Cdkal1* KO mice, and that it was normally expressed in WT mice ($p < 0.001$; Fig. 9A, 9B). Next, as a result of confirming the expression levels of EL and HL proteins known to be involved in HDL

remodeling in blood, it was confirmed that the two lipases were significantly decreased in the *Cdkal1* KO group ($p = 0.002$, $p<0.001$ versus WT mice; Fig. 9B). It can be seen that the decrease in HDL remodeling-related proteins leads to an increase in HDL particle size. ABCA1 and SR-B1 protein levels, which directly affect cholesterol efflux, were also identified. ABCA1 levels did not change between *Cdkal1* KO mice and WT mice ($p > 0.05$; Fig. 9B). However, the expression level of SR-B1 protein, which plays a key role in RCT by acting as a HDL receptor in the liver, was significantly increased in *Cdkal1* KO mice compared to that in WT mice ($p = 0.007$; Fig. 9B).

Among the three proteins (EL, HL, SR-B1) that showed significant changes in *Cdkal1* KO mouse liver tissue, which protein had a direct effect was confirmed through the correlation between cholesterol efflux and protein expression. As a result of correlation analysis by the Pearson correlation coefficient method, it was confirmed that SR-B1 among the three proteins had a significant effect on cholesterol efflux ($p < 0.05$; Fig. 10). Together, these studies suggest that liver-specific *Cdkal1* reduction may reduce atherosclerosis by promoting cholesterol efflux through increased SR-B1 expression.

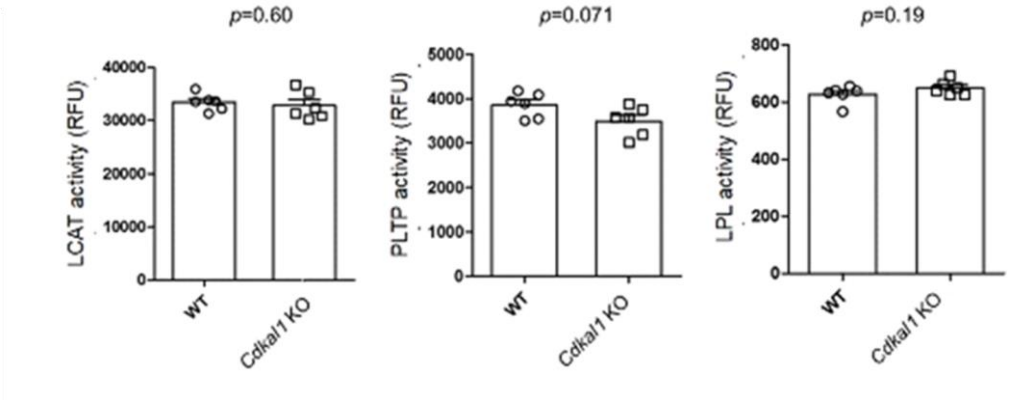

Figure 8. Enzyme activities in *Cdkal1* KO mouse plasma. The enzyme activities of LCAT, PLTP, and LPL, which are enzymes that act on the cholesterol metabolism process, were confirmed in *Cdkal1* KO mouse and WT mouse plasma (n = 6 in each group). 8-week-old mice plasma samples were obtained and subjected to LCAT, PLTP, LPL activity tests as described in materials and methods. Results were presented with mean ± SEM. Statistical analysis by permutation test.

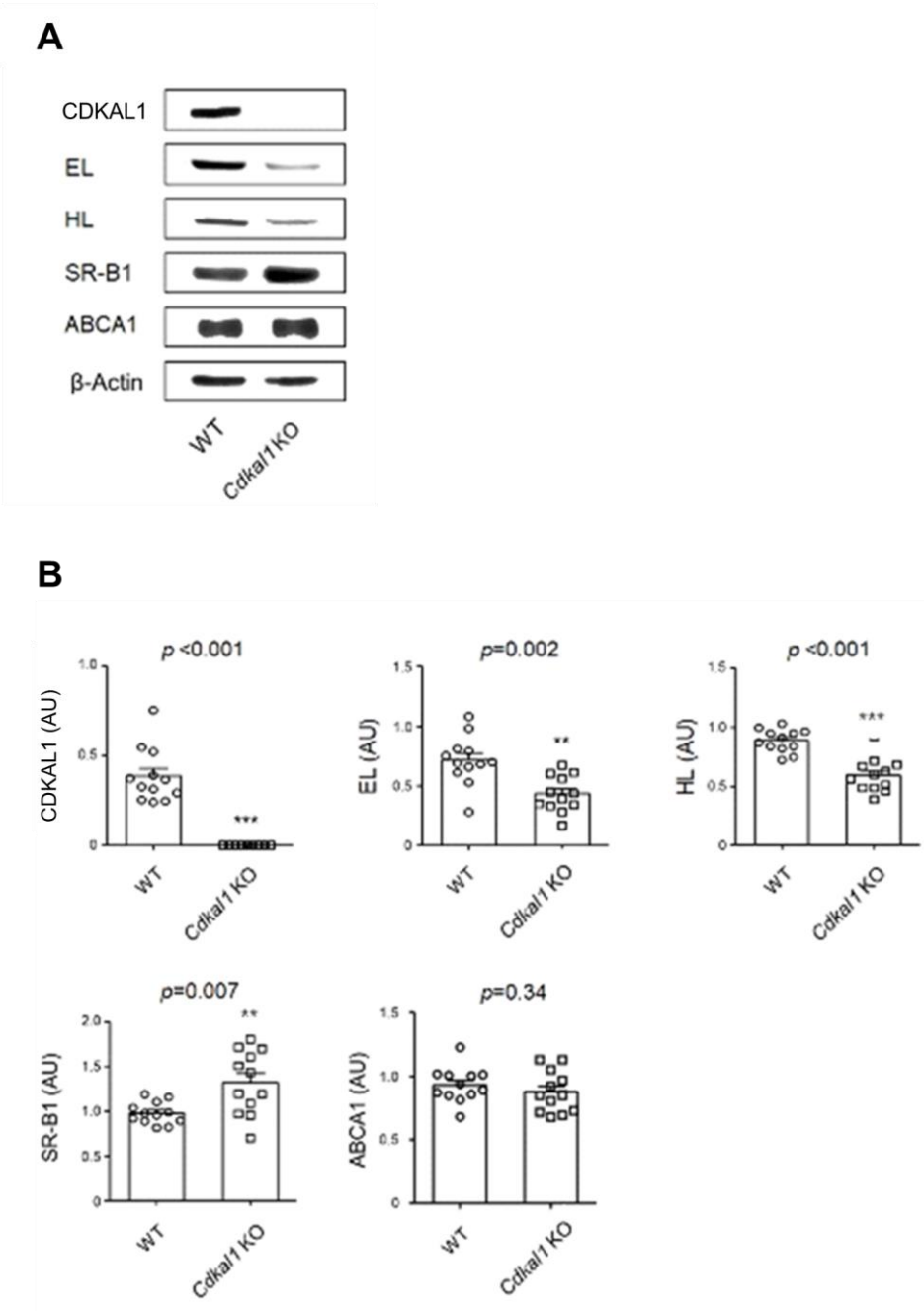

Figure 9 legend (the following page)

Figure 9. Hepatic *Cdkal1* deletion regulates SR-B1, EL, and HL protein levels in liver tissue. Western blot analysis of CDKAL1, EL, HL, SR-B1, and ABCA1. Expression of HDL metabolism-related proteins in liver extracts of 8-week-old *Cdkal1* KO mice was confirmed by immunoblotting after electrophoresis (Compared to WT mice; n =12 in each group). (A) Representative image of western blot of liver tissue. (B) Graph quantifying western blot images using Image J program. Results were presented with mean±SEM. $^{**}p < 0.01$, and $^{***}p < 0.001$ compared with WT (Permutation test).

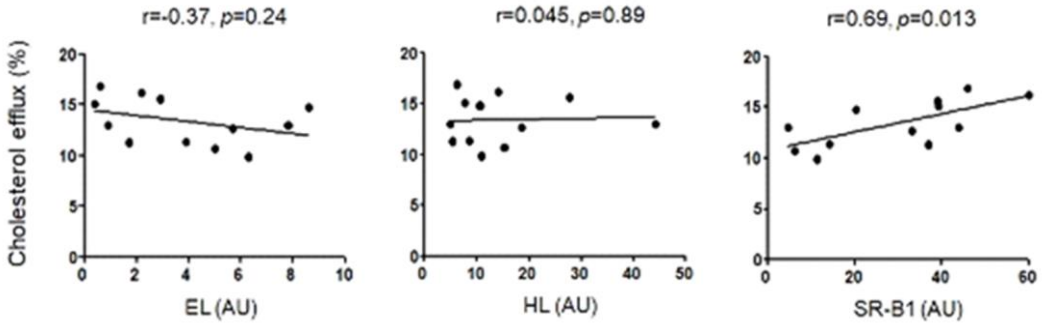

Figure 10. Correlation between cholesterol efflux and proteins involved in HDL metabolism. Statistical identification of the correlation between SR-B1, EL, and HL protein expression and CEC used the Pearson correlation coefficient. Results were presented with mean ± SEM. *$p < 0.05$ (Pearson correlation coefficient).

3.5. Differentially expressed genes and related pathways

Hepatocytes obtained from WT and *Cdkal1* KO mice were used for RNA sequencing. Differentially expressed genes and related pathways were analyzed as described in the Methods section. A volcano plot displayed 278 and 65 genes that were up- and downregulated, respectively, in seven *Cdkal1* KO mice compared to their levels in WT mice (Fig. 11A). The top ten up- and downregulated genes are presented based on KEGG enrichment analysis in Figure B. Upregulated genes included *Lrp2* and *Fxyd2,* whereas downregulated included *Cel* and *Prss2* (Fig. 11B). Further analysis identified pathways related to up- and downregulated genes in *Cdkal1* KO mice. Interestingly, the bile secretion pathway was highly ranked among the upregulated pathways (Fig. 11C).

A

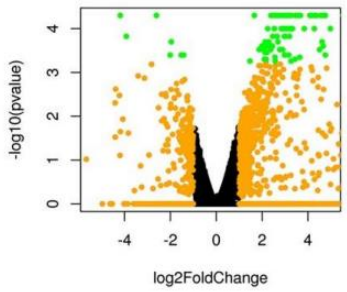

B

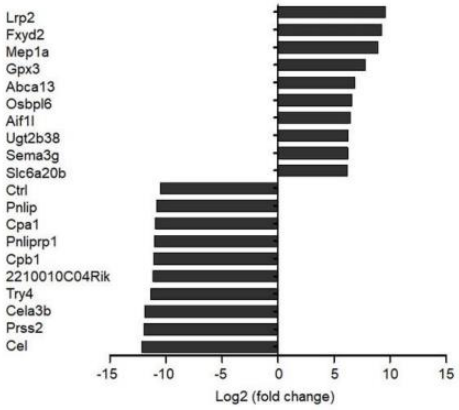

C

Upregulated pathways	*p*	Downregulated pathways	*p*
Protein digestion and absorption	1.20E-07	Systemic lupus erythematosus	4.91E-28
Aldosterone-regulated Na reabsorption	3.97E-06	Alcoholism	1.76E-24
Bile secretion	8.86E-05	Viral carcinogenesis	1.20E-11
Mineral absorption	2.22E-04	Protein digestion and absorption	3.47E-10
Proximal tubule bicarbonate reclamation	5.83E-04	Pancreatic secretion	1.99E-09

Figure 11 legend (the following page)

Figure 11. Analysis of gene set in RNA sequencing data of hepatocytes from liver-specific *Cdkal1* KO mice.

(A) A volcano plot showing differentially expressed genes in *Cdkal1* KO mice versus wild-type mice. Yellow and green points represent expression levels of genes significantly up- or downregulated, respectively, in the KO mice compared to their levels in the controls. The x- and y-axes indicate $\log_2$ fold-changes in the expression and log odds of differentially expressed genes, respectively. (B) Top ten up- and downregulated genes in hepatocytes from *Cdkal1* KO mice. KEGG pathway analysis was performed for functional enrichment clustering. A total of 343 genes were differentially expressed in hepatocytes from *Cdkal1* KO mice. Top-ranked genes are shown among 278 upregulated and 65 downregulated genes. (C) Pathways associated with differentially expressed genes in *Cdkal1* KO mice. The top five up- and downregulated pathways identified in KEGG pathway classification are presented.

IV. DISCUSSION

In this study, we found that liver-specific *Cdkal1* deficiency promoted CEC independently of plasma lipid profile levels. Deletion of *Cdkal1* in mice model of diet-induced atherosclerosis showed a trend of decreasing the size of the lesion. In addition, deletion of *Cdkal1* in the liver suppressed EL and HL protein secretion and increased SR-B1 expression. RNA sequencing analysis of mouse hepatocytes confirmed that the bile secretion pathway was upregulated in hepatocytes of *Cdkal1* KO mice to confirm the exact pathway by which the *Cdkal1* gene affects CEC. These findings provide an *in vivo* evidence of the possibility that genetic deletion of liver-specific *Cdkal1* may promote CEC and attenuate atherosclerosis through increased SR-B1 expression in mice.

We identified, for the first time, the mechanism by which *Cdkal1* affects CEC. As expected, we confirmed that *Cdkal1* deletion increased macrophage cholesterol CEC *in vitro* in *Cdkal1* KO mouse plasma compared to that in WT mouse plasma. Cholesterol efflux from macrophages is the first step in RCT to alleviate atherosclerosis [12] increasing CEC in *Cdkal1* KO mice would have a positive effect on cholesterol metabolism *in vivo*. In order to identify the mechanism by which *Cdkal1* affects CEC, we measured the activity of several enzymes (such as LCAT, PLTP, LPL) and protein (EL, HL, ABCA1, SR-B1) that play an important role in HDL remodeling. As a result, the enzyme activity was not changed, but the lipase protein, which regulates HDL size and liver absorption, was significantly decreased. This result means that the mature HDL is not absorbed by the liver and continues to stay in the blood vessel as a large-sized HDL. In addition, ABCA1 protein, which plays

a role in transferring cholesterol from macrophages to HDL, was not changed in *Cdkal1* KO mice, but SR-B1 protein, which is known to selectively absorb cholesterol from HDL in the liver, was increased in *Cdkal1* KO liver tissue. Therefore, HDL of large size is not eliminated or converted to small size by lipase reduction, but lipid removal in HDL is promoted by increased SR-B1. It has been reported that a large-sized HDL that stays in the bloodstream can uptake more lipids than a small-sized HDL, and that it has a positive effect on atherosclerosis [8–10] Our experimental results suggested a previously unreported association between liver *Cdkal1* deletion and SR-B1, EL and HL. Other studies have shown that SR-B1 plays an important role in cholesterol metabolism, but overexpression of the SR-B1 protein increases RCT but decreases HDL levels [23, 24]. Also, it has been thought that EL and HDL levels are inversely proportional and have a negative effect on RCT. However, the effect of EL-mediated HDL levels on atherogenesis remains controversial. Previous reports have shown *in vivo* that when EL is overexpressed in the liver, HDL is reduced but cholesterol reverse transport ability is maintained [20]. This is consistent with our experimental data highlighting that HDL function and cholesterol flux are ultimately more positive factors of atherosclerosis than absolute HDL-C concentrations.

Next, we presented the potential for liver-specific *Cdkal1* KO to ameliorate atherosclerosis. *Apoe/Cdkal1* KO mice were generated for atherosclerosis induction and then atherosclerosis was induced by HCD. As a result, the size of atherosclerotic lesions tended to decrease in mice in which the *Cdkal1* gene was removed from the liver, but there was no significant difference. This result is thought to be due to atherosclerosis induced by

a high-cholesterol diet for too long, despite the increase in CEC caused by *Cdkal1* deletion. Therefore, in order to examine the effect of *Cdkal1* gene deletion on the early stage and progression of atherosclerosis, detailed inflammatory response and various histological analyzes are needed in the lesion tissue and further experiments are being planned with an appropriate model that does not include an excessive diet induction period. Interestingly, the bile secretion pathway was highly ranked among the upregulated pathways as a result of RNA sequencing analysis to confirm the specific mechanism by which the SR-B1 protein increases when *Cdkal1* deficiency in the liver. Based on these RNA sequencing results, we plan to investigate the mechanism between *Cdkal1* and CEC in more detail through additional experiments.

In this study, we could not determine which pathway *Cdkal1* deficiency affects SR-B1, EL, and HL, and there was no significant difference in the effect of liver-specific Cdkal1 deletion on atherosclerosis. Therefore, it is difficult to expect *Cdkal1* as a unique therapeutic target for atherosclerosis, but nevertheless, this study is the first to show that liver-specific deletion of *Cdkal1* in mice affects regulated protein expression related to HDL catabolism and promotes CEC.

Taken together, we constructed liver-specific *Cdkal1* KO mice and demonstrated for the first time that reduction of *Cdkal1* regulates the expression of SR-B1, EL, and HL proteins in liver tissue and promotes CEC. Surprisingly, it was confirmed that, among them, SR-B1 was significantly correlated with CEC. HDL catabolic protein regulation by *Cdkal1* inhibition could be a novel therapeutic target for atherosclerosis. Further research is needed

to elucidate the specific mechanisms supporting this association.

REFERENCES

1. Yang, Y. et al. High-density lipoprotein cholesterol and the risk of myocardial infarction, stroke, and cause-specific mortality: a nationwide cohort study in Korea. J. Lipid Atheroscler. 10, 74–87 (2021).

2. Cho, Y. K. & Jung, C. H. HDL-C and cardiovascular risk: you don’t need to worry about extremely high HDL-C levels. J. Lipid Atheroscler. 10, 57–61 (2021).

3. Holmes, M. V. et al. Mendelian randomization of blood lipids for coronary heart disease. Eur. Heart J. 36, 539–550 (2015).

4. Schwartz, G. G. et al. Effects of dalcetrapib in patients with a recent acute coronary syndrome. N. Engl. J. Med. 367, 2089–2099 (2012).

5. Zhao, Q. et al. A Mendelian randomization study of the role of lipoprotein subfractions in coronary artery disease. ELife. 10, e58361 (2021).

6. OTVOS, James D. Measurement of lipoprotein subclass profiles by nuclear magnetic

resonance spectroscopy. Clin Lab. 48, 171-80 (2002).

7. El Harchaoui, K. et al. High-density lipoprotein particle size and concentration and coronary risk. Ann Intern Med. 150, 84-93 (2009).

8. Van der Steeg, W. A., Holme, I., Boekholdt, S. M., Larsen, M. L, Lindahl, C, Stroes, E. S, et al. High-density lipoprotein cholesterol, high-density lipoprotein particle size, and apolipoprotein AI: significance for cardiovascular risk: the IDEAL and EPIC-Norfolk studies. J Am Coll Cardiol. 51, 634-642 (2008).

9. Mora, S., Otvos, J. D., Rifai, N., Rosenson, R. S., Buring, J. E., and Ridker, P. M., et al. Lipoprotein particle profiles by nuclear magnetic resonance compared with standard lipids and apolipoproteins in predicting incident cardiovascular disease in women. Circulation, 119, 931-939 (2009).

10. George, R. T. et al. MEDI6012: recombinant human lecithin cholesterol acyltransferase, high-density lipoprotein, and low-density lipoprotein receptor-mediated reverse cholesterol transport. J. Am. Heart Assoc. 10, e014572 (2021).

11. Kingwell, B. A. et al. Antiatherosclerotic effects of CSL112 mediated by enhanced cholesterol efflux capacity. J. Am. Heart Assoc. 11, e024754 (2022).

12. Chiesa, Scott T, Marietta Charakida, et al. High-density lipoprotein function and dysfunction in health and disease. Cardiovascular drugs and therapy 332, 207-219 (2019).

13. Cheon, E. J. et al. Novel association between CDKAL1 and cholesterol efflux capacity: replication after GWAS-based discovery. Atherosclerosis 273, 21–27 (2018).

14. Lee, H. A., Park, H. & Hong, Y. S. Sex differences in the effects of CDKAL1 variants on glycemic control in diabetic patients: findings from the Korean genome and epidemiology study. Diabetes Metab. J. Preprint at https://doi.org/10.4093/dmj.2021.0265 (2022).

15. Vassilis I Zannis, Panagiotis Fotakis, et al. HDL biogenesis, remodeling, and catabolism. Handb Exp Pharmacol. 224, 53-111 (2015).

16. Edmondson, Andrew C., et al. Dense genotyping of candidate gene loci identifies

variants associated with high-density lipoprotein cholesterol. Circ Cardiovasc Genet. 4, 145-155 (2011).

17. Jin, Weijun, et al. Inhibition of endothelial lipase causes increased HDL cholesterol levels in vivo. J Clin Invest. 111, 357-362 (2003).

18. OUIMET, Mireille; BARRETT, Tessa J.; FISHER, Edward A. HDL and reverse cholesterol transport: Basic mechanisms and their roles in vascular health and disease. Circ Res. 124, 1505-1518 (2019).

19. S. Mweva, J.L. Paul, M. Cambillau, et al. Comparison of different cellular models measuring in vitro the whole human serum cholesterol efflux capacity. Eur J Clin Invest. 36, 552-559 (2006).

20. Takiguchi, Shunichi, et al. Hepatic overexpression of endothelial lipase lowers high-density lipoprotein but maintains reverse cholesterol transport in mice: role of scavenger receptor class B type I/ATP-binding cassette transporter A1-dependent pathways. Arterioscler Thromb Vasc Biol. 38, 1454-1467 (2018).

21. Oldoni, Federico; SINKE, Richard J.; KUIVENHOVEN, Jan Albert. Mendelian disorders of high-density lipoprotein metabolism. Circ Res. 114, 124-142 (2014).

22. Miwa, Kenji, et al. Cholesterol efflux from J774 macrophages and Fu5AH hepatoma cells to serum is preserved in CETP-deficient patients. Clin Chim Acta. 402, 19-24 (2009).

23. Duffy, Danielle; RADER, Daniel J. Update on strategies to increase HDL quantity and function. Nat Rev Cardiol. 6, 455-463 (2009).

24. Zhang, YuZhen, et al. Hepatic expression of scavenger receptor class B type I (SR-BI) is a positive regulator of macrophage reverse cholesterol transport in vivo. J Clin Invest. 115, 2870-2874 (2005).

ABSTRACT (IN KOREAN)

간 Cdka11 결실이 고밀도지단백 대사 변화를 통해 콜레스테롤 유출능 향상에 미치는 효과

<지도교수 이상학>

연세대학교 대학원 노화과학협동과정

안단비

이전 연구에서 *CDKAL1*유전자의 특정 부위에 변이가 있는 환자는 CEC가 촉진된다고 보고되었습니다. *CDKAL1* 유전자는 당뇨병 위험인자로 알려져 있지만 현재까지 정확한 콜레스테롤 대사에 대한 영향을 확인한 연구는 없었습니다.

이 연구에서 우리는 콜레스테롤 대사에 대한 *Cdka11* 유전자의 효과를 *Cdka11*유전자가 간특이적으로 제거된 마우스(*Cdka11* KO)에서 확인하였습니다.

Cdka11 KO 마우스와 WT 마우스 혈장에서 혈당과 지질 프로필은 두 그룹 간에 차이가 없었습니다. 하지만, CEC는 WT 마우스보다 *Cdka11* KO 마우스에서 더 높았고(p=0.007) *Apoe* KO 마우스보다 *Apoe/Cdka11* KO 마우스에서 더 높았습니다(p=0.034).

다음으로, 우리는 간에서 *Cdka11*의 제거가 어떤 경로로 CEC를 촉진시키는지 확인하기 위해, 콜레스테롤 대사에 핵심적인 역할을 하는 단백질을 Western blotting으로 확인한 결과, *Cdka11* KO 마우스에서 감소된 EL(p=0.002), HL(p<0.001) 및 증가된 SR-B1(p=0.007)단백질 양을 보여주었습니다. 또한, HDL-C 이화작용에 영향을 주는 LCAT, PLTP 및 LPL의 활성을 확인한 결과 WT와 *Cdka11* KO 마우스 간에 유사했습니다.

마지막으로 간에서 *Cdka11* 유전자 결핍이 실제 죽상동맥경화 완화에 도움이 되는지 확인하기위해 *Apoe/Cdka11* KO 마우스와 *Apoe* KO 마우스를 16주동안 고콜레스테롤 식이를 먹인 뒤 병변 크기를 Oil Red O 염색을 통해 확인하였습니다. 그 결과 *Apoe/Cdka11* KO 군에서 병변 크기가 감소하는 경향을 보였으나 (p<0.067), 유의한 차이는 확인하지 못했습니다. 타겟분석에서 놓친 Cdka11유전자가 CEC에 영향을 주는 추가 경로를 확인하기위해 마우스 간세포를 RNA sequencing분석한 결과 Cdka11 KO마우스의 간세포에서 담즙 분비 경로가 상향 조절 되는 것을 확인했습니다.

현재 연구는 HDL 이화작용을 위한 단백질 조절과 함께 *Cdka11*의 간 특이적 결실이 있는 마우스에서 CEC 가 촉진된다는 것을 처음으로 입증했습니다. 이 연구는 *CDKAL1*이 HDL 기능과 혈관 병리를 개선하기 위한 중재의 표적이 될 수 있음을 시사합니다.

핵심되는 말: 고밀도지단백, 동맥경화, 대식세포, 간